

1 Characteristics and degradation of organic aerosols from cooking  
2 sources based on hourly observation of organic molecular markers in  
3 urban environment

4  
5 Rui Li <sup>a, b#</sup>, Kun Zhang <sup>a, b#</sup>, Qing Li <sup>a, b</sup>, Liumei Yang <sup>a, b</sup>, Shunyao Wang <sup>a, b</sup>, Zhiqiang Liu <sup>a, b, c</sup>, Xiaojuan Zhang <sup>a, b,</sup>  
6 <sup>c</sup>, Hui Chen <sup>a, b</sup>, Yanan Yi <sup>a, b</sup>, Jialiang Feng <sup>a, b</sup>, Qiongqiong Wang <sup>d</sup>, Ling Huang <sup>a, b</sup>, Wu Wang <sup>a, b</sup>, Yangjun Wang <sup>a,</sup>  
7 <sup>b</sup>, Jian Zhen Yu <sup>e, f</sup>, Li Li <sup>a, b\*</sup>

8  
9 <sup>a</sup> School of Environmental and Chemical Engineering, Shanghai University, Shanghai, China

10 <sup>b</sup> Key Laboratory of Organic Compound Pollution Control Engineering (MOE), Shanghai University, Shanghai, China

11 <sup>c</sup> Jiangsu Changhuan Environment Technology Co., Ltd., Changzhou, Jiangsu, China

12 <sup>d</sup> School of Environmental Studies, China University of Geosciences, Wuhan, 430074, China

13 <sup>e</sup> Department of Chemistry, Hong Kong University of Science & Technology, Hong Kong, China

14 <sup>f</sup> Division of Environment & Sustainability, Hong Kong University of Science & Technology, Hong Kong, China

15  
16 # These two authors contributed equally to this work.

17 \* Correspondence: Li Li (Lily@shu.edu.cn)

18 **Abstract**

19 Molecular markers in organic aerosol (OA) provide specific source information of PM<sub>2.5</sub>, and the contribution of  
20 cooking organic aerosols to OA is significant, especially in urban environments. However, the low time resolution of offline  
21 measurements limits the effectiveness in interpreting the tracer data, the diurnal variation of cooking emission and the  
22 oxidation process. In this study, we used on-line thermal desorption aerosol gas chromatography mass spectrometry (TAG)  
23 to measure organic molecular markers in fine particulate matter (PM<sub>2.5</sub>) at an urban site in Changzhou, China. The  
24 concentrations of saturated fatty acids (sFA), unsaturated fatty acids (uFAs), and oxidative decomposition products of  
25 unsaturated fatty acids (ODPs) were measured every two hours to investigate the temporal variations and the oxidative  
26 decomposition characteristics of uFAs in urban environment. The average concentration of total fatty acids (TFAs, sum of  
27 sFAs and uFAs) was measured to be 105.70± 230.28 ng/m<sup>3</sup>. The average concentration of TFAs in polluted period (PM<sub>2.5</sub>

28  $\geq 35 \mu\text{g}/\text{m}^3$ ) was  $147.06 \text{ ng}/\text{m}^3$ , which was 4.2 times higher than that in clean period ( $\text{PM}_{2.5} < 35 \mu\text{g}/\text{m}^3$ ), higher than the  
29 enhancement of  $\text{PM}_{2.5}$  (2.2 times) and organic carbon (OC) (2.0 times) concentrations comparing polluted period to clean  
30 period. The mean concentration of cooking aerosol in the polluted period ( $4.0 \mu\text{g}/\text{m}^3$ ) was about 5.3 times higher than that  
31 in the clean period ( $0.75 \mu\text{g}/\text{m}^3$ ), which was similar to the trend of fatty acids. Fatty acids showed a clear diurnal variation.  
32 Linoleic acid /stearic acid and oleic acid / stearic acid ratios were significantly higher at dinner time, and closer to the  
33 cooking source profile. By performing backward trajectory clustering analysis, under the influence of short-distance air  
34 masses from surrounding areas, the concentrations of TFAs and  $\text{PM}_{2.5}$  were relatively high; while under the influence of  
35 air masses from easterly coastal areas, the oxidation degree of uFAs emitted from local culinary sources were higher. The  
36 effective rate constants ( $k_O$ ) for the oxidative degradation of oleic acid were estimated to be  $0.08\text{-}0.57 \text{ h}^{-1}$ , which were lower  
37 than  $k_L$  (the estimated effective rate constants of linoleic acid,  $0.16\text{-}0.80 \text{ h}^{-1}$ ). Both  $k_O$  and  $k_L$  showed a significant positive  
38 correlation with  $\text{O}_3$ , indicating that  $\text{O}_3$  was the main night-time oxidants for uFAs in the Changzhou City. Using fatty acids  
39 as tracers, cooking was estimated to contribute an average of 4.6% to  $\text{PM}_{2.5}$  concentrations, increased to 7.8% at 20:00.  
40 Cooking was an important source to OC, contributing to 8.1%, higher than the contribution to  $\text{PM}_{2.5}$ . This study investigates  
41 the variation of the concentrations and oxidative degradation of fatty acids and corresponding oxidation products in ambient  
42 air, which can be a guide for the refinement of aerosol source apportionment, and provide scientific support for the  
43 development of cooking source control policies.

## 44 1. Introduction

45 Organic aerosol (OA) is an important component of fine particulate matter ( $\text{PM}_{2.5}$ ), accounting for 20-90% of the total  
46  $\text{PM}_{2.5}$  mass (Kanakidou et al., 2005). Among different OA sources, restaurant fumes are relatively important (Huang et al.,  
47 2021). The contribution of cooking organic aerosols (COA) to OA is significant, especially in urban environments, where  
48 COA can contribute 11%-34% to total organic carbon (OC) and 3%-9% to  $\text{PM}_{2.5}$  mass concentration, even higher than  
49 traffic-related hydrocarbon-based OA (Huang et al., 2021; Li et al., 2020). The presence of carcinogenic mutagens in  
50 restaurant fumes contains chemicals that can be harmful to human immune function (Huang et al., 2020). According to the  
51 2018 global cancer statistics, lung cancer accounts for 24.1% of all cancer deaths in China and is the most common cause  
52 of cancer-related deaths in China. The carcinogenic risk analysis suggested that the potentially adverse health effects  
53 induced by cooking sources should not be ignored (Zhang et al., 2017a).

54 Cooking is an important source contributor to  $\text{PM}_{2.5}$ , especially in urban environments. Cooking sources have recently  
55 received increasing attention, but they are largely an uncontrolled source of  $\text{PM}_{2.5}$ . Saturated fatty acids (sFAs) and

56 unsaturated fatty acids (uFAs), such as palmitic, stearic, and oleic acids, are known molecular markers from cooking  
57 emissions, which are released primarily during cooking activities from the hydrolysis and thermal oxidation of cooking  
58 oils. Fatty acids and their derivatives are often used as tracers in the receptor model for the source apportionment of PM<sub>2.5</sub>.  
59 It has been found that nonanoic acid, 9-oxononanoic acid and azelaic acid are the main atmospheric oxidation products  
60 of oleic acid in the aerosol, while uFAs such as oleic and linoleic acids also react with other atmospheric oxidants, such as  
61 hydroxyl (OH) (Nah et al., 2014; Wang et al., 2020).

62 In previous studies on the molecular tracers of cooking source based on filter membrane sampling, the time resolution  
63 usually varies from one day to several days, which cannot accurately capture the diurnal variations of pollutants emitted  
64 by the cooking source (Li et al., 2021). The thermal desorption aerosol gas chromatography–mass spectrometry (TAG)  
65 enables online monitoring of organic molecular markers (Wang et al., 2020). By clarifying the characteristics of cooking  
66 emissions, quantifying the concentrations of pollutants emitted from cooking and its contribution to urban OA on the  
67 diurnal time scales, we build up data and process knowledge about cooking-source PM<sub>2.5</sub> pollution, which in turn help us  
68 to evaluate the option of controlling cooking emissions in the overall pollution prevention for urban environments.

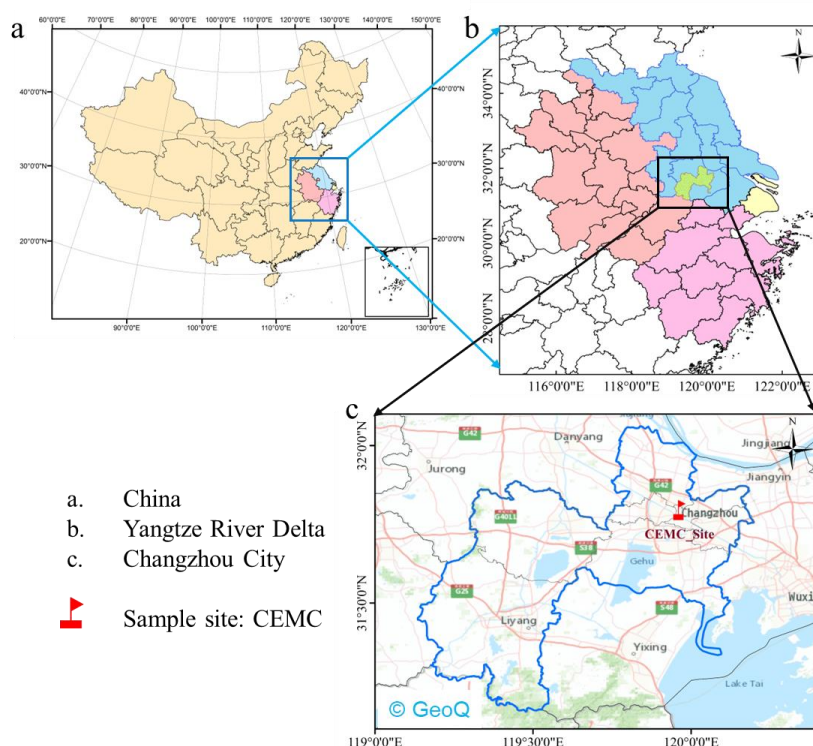
69 Processes such as emission rate, atmospheric dilution, and photochemical oxidation can affect aerosol composition  
70 measured at receptor sites (Fortenberry et al., 2019; Yee et al., 2018). Particulate organic matter can undergo heterogeneous  
71 oxidation by ozone, OH and nitrate (NO<sub>3</sub>) radicals (Wang et al., 2020). When using organic tracer data from filter analysis,  
72 variations in concentration due to degradation or secondary production were reported (Ringuet et al., 2012). These  
73 degradation and generation processes in the atmosphere are therefore worthy of our attention when using organic markers  
74 as source tracers. The mechanism and kinetics of ozonolysis of oleic acid and linoleic acid in the presence of oxidants such  
75 as NO<sub>3</sub>, O<sub>3</sub> and OH radicals have been extensively studied in the laboratory studies (Vesna et al., 2009; Zahardis and  
76 Petrucci, 2007; Ziemann, 2005). The aging of POA markers under atmospheric conditions, however, is still far from being  
77 properly understood with few field observations performed in this topic compared to laboratory studies (Bertrand et al.,  
78 2018a; Bertrand et al., 2018b). The high timely-resolved observations would help to fill this gap.

79 In this study, TAG was employed at an urban site in Changzhou, China, to investigate the variation of atmospheric  
80 cooking-related fatty acids with hourly resolution data (Ren et al., 2019). The aim of this study is to identify the contribution  
81 of cooking emissions to ambient PM<sub>2.5</sub> with hourly organic molecular data and to investigate the oxidative decomposition  
82 reactions of cooking-related uFAs in an urban area. Results of this study could provide valid basis and insights for the  
83 refinement of PM<sub>2.5</sub> source apportionment as well as atmospheric modelling.

## 84 2. Methodology

### 85 2.1 Field measurement

86 Gaseous pollutants, PM<sub>2.5</sub> and its main chemical constituents (water soluble ions, carbon components and elements,  
87 etc.) as well as organic markers (alkanes, hopanes, polycyclic aromatic hydrocarbons, sugars, alcohols and organic acids,  
88 etc.) were measured online at the Changzhou Environmental Monitoring Center of Jiangsu Province (CEMC) (31.76N,  
89 119.96E) during January-March 2021, which is a representative urban site (Fig. 1). The meteorological parameters were  
90 obtained from a meteorological monitor (WXT520, VAISALA Inc., FL). O<sub>3</sub> and NO<sub>2</sub> were measured by ozone analyzer  
91 (49i-PS, Thermo Fisher Scientific, US) and NO<sub>x</sub> analyzer (MODEL450i, Thermo Fisher Scientific, US), respectively.  
92 PM<sub>2.5</sub> mass concentration was measured by an online particulate matter monitor (BAM1020, Met One Inc., US); the  
93 concentration of the carbon components (Organic carbon, OC; Elemental carbon, EC) was measured using semi-continuous  
94 OC/EC analyzer (RT-4, Sunset Laboratory Inc, US) (Nicolosi et al., 2018; Zhang et al., 2017b); water soluble ions were  
95 measured by MARGA ionic online analyzer (ADI2080, Metrohm, CHN) (Makkonen et al., 2012) and elements were  
96 measured by an atmospheric elements online monitor (EHM-X200, Tianrui, CHN) (Makkonen et al., 2012).



97  
98 **Figure 1. Location of the sampling site in Changzhou, China.**

99 Quantification of hourly speciated organic markers was achieved using TAG. The operation details and data quality  
100 have been described in our previous work (Wang et al., 2020; Zhang et al., 2021). The sampling and analysis sequence of

101 the TAG system includes four steps: (a) PM<sub>2.5</sub> sampling and synchronous gas chromatography-mass spectrometry (GC-  
102 MS) analysis of the previous sample; (b) loading of the internal standards (IS) from the standards (STD) reservoir to a  
103 thermal desorption cell; (c) derivatization and thermal desorption of analytes on the collection and thermal desorption  
104 (CTD) cell and subsequent preconcentration of the analytes in focusing trap (FT); and (d) loading of analytes into the GC  
105 column for GC-MS analysis. The following is a detailed description. Ambient air was sampled at a flow rate of 8.5-9.5  
106 L/min through a cyclone with PM<sub>2.5</sub> cutting size (BGI Inc., Waltham, MA), a Nafion dryer (PERMA PURE, MD-700-24S-  
107 3) to remove moisture, and then through a carbon denuder (model: ADI-DEN2) to remove volatile organics. The sampled  
108 particles were collected on the CTD cell at 30°C for 60 min, followed by derivatization and thermal desorption for 8 min  
109 as the temperature of the CTD cell increases to 300°C in 2 min and maintains for 6 min, during which a 10 mL/min helium  
110 purge flow combined with a 40 mL/min derivatization flow with N-methyl- N-(trimethylsilyl) trifluoroacetamide (MSTFA)  
111 flow through for 8 min. Subsequently, the FT was heated to 300°C in 2 min and kept at 300°C for 10 min, transferring the  
112 analytes onto the GC column head (DB-5MS, size 30 m × 0.25 μm × 0.25 μm) by carrier gas. After GC separation, the  
113 target organics were sent to the MS detector for quantification. The GC-MS analysis duration for each sample was 60 min  
114 while collection of the next sample the CTD cell starts. With the current TAG instrumental set-up, samples were collected  
115 every even hour. The post-sampling steps, including in-situ derivatization, thermal desorption, GC-MS analysis, and  
116 standby step, took 2 h, thus producing 12 samples per day.

117 The summary of target organic molecular markers and IS are shown in Table 1. Identification of compounds was  
118 performed by comparing retention times and mass spectra with those of authentic standards ([Vesna et al., 2009](#); [Wang et  
119 al., 2020](#)). Calibration curves were established by internal standard method. The correlation coefficients of the calibration  
120 curves range from 0.88-1.00. For compounds without authentic standards and for compounds whose authentic standards  
121 are not included in the current standard mixture, their identification is performed by comparing their mass spectra with the  
122 National Institute of Standards and Technology (NIST) libraries. Azelaic acid was identified and quantified by using  
123 authentic standards. Nonanoic acid and 9-oxononanoic acid were identified by comparison with mass spectra in the NIST  
124 library and by referring to [Ziemann \(2005\)](#), [Pleik et al. \(2016\)](#) and [Wang et al. \(2020\)](#). Ozone oxidation of oleic acid yields  
125 C<sub>9</sub> aldehydes and acids including nonanal, azelaic acid, nonanoic acid, and 9-oxononanoic acid. Since nonanal could also  
126 be primary in the gas phase, it is thus not discussed in this paper. The library of the NIST was identified and quantified  
127 using the alternative standards specified in Table 1.

128  
129

130 **Table 1. Statistics of hourly concentrations of organics associated with cooking emissions measured by TAG during the**  
 131 **campaign.**

Compounds	Average	Stdev	Min	Max	Quantification IS
Myristic acid <sup>a</sup>	0.69	1.33	0.03	10.14	Palmitic acid-d <sub>31</sub>
Palmitic acid	38.77	84.14	1.45	670.12	Palmitic acid-d <sub>31</sub>
Stearic acid	26.51	50.58	1.81	341.65	Palmitic acid-d <sub>31</sub>
Oleic acid	32.15	81.34	0.96	723.95	Stearic acid-d <sub>35</sub>
Linoleic acid <sup>b</sup>	7.80	28.32	0.09	326.50	Stearic acid-d <sub>35</sub>
Nonanoic acid <sup>c</sup>	1.19	1.32	BD <sup>d</sup>	7.94	Adipic acid-d <sub>10</sub>
9-oxononanoic acid <sup>c</sup>	3.91	4.73	0.19	17.18	Adipic acid-d <sub>10</sub>
Azelaic acid	9.15	32.99	BD	309.64	Adipic acid-d <sub>10</sub>

a, Quantified using palmitic acid as the surrogate; b, Quantified using oleic acid as the surrogate; c, Quantified using azelaic acid as the surrogate; d, Below detection limit.

## 132 2.2 Backward trajectory analysis

133 Backward trajectory analysis is a useful tool in identifying the influence of air masses on the chemical composition  
 134 of PM<sub>2.5</sub> (Wang et al., 2017). Backward trajectories of 36-h duration arriving at an altitude of 100 m above ground level  
 135 (AGL) over the CEMC site were calculated deploying the 0.5° Global Data Assimilation System (GDAS) meteorological  
 136 data (<https://www.ready.noaa.gov/archives.php>, last access: Aug 16, 2022). The trajectories were then classified into  
 137 different clusters according to the geographical origins and movement of the trajectories using the TrajStat model (Li et al.,  
 138 2020).

## 139 2.3 Relative rate constant analysis

140 Ambient concentrations of species are influenced by its emissions, atmospheric dilution/compaction, chemical  
 141 loss/production, and wet/dry deposition. As the target sFAs and uFAs in urban environments are predominately primary in  
 142 their source origin, the chemical production rate could be assumed to be negligible. Donahue et al. (2005) formulated the  
 143 relative rate expression for heterogeneous oxidation reactions of multicomponent OA. The specific expression applied to  
 144 the ambient measurements of uFAs is derived, as given in Equation (Eq 1) and Equation (Eq 2) (Wang and Yu, 2021).

$$145 \quad \frac{C_i}{C_s} = A \times e^{-kt} \quad (1)$$

$$146 \quad k \approx k_{r_i} \times C_{OX} \quad (2)$$

147  $C_i$  and  $C_s$  are the particle-phase concentration of species  $i$  and sFAs, respectively. Among the quantified sFA and uFA  
 148 cooking markers, palmitic acid was selected as the reference molecule for normalization. Using the concentration ratio  
 149 eliminates the interference from atmospheric dilution and deposition. Fitting the ambient  $C_i/C_s$  data versus  $t$  with an  
 150 exponential function provides an estimate for  $k$ , the effective pseudo-first order decay rate ( $\text{h}^{-1}$ ).  $k_{r_i}$  is the second-order  
 151 reaction rate constant of species  $i$  against an oxidant.  $C_{OX}$  is the average oxidant concentration in the aerosol.

## 152 2.4 Source apportionment based on PMF

153 Positive Matrix Factorization (PMF) is a bilinear factor analysis method, which is widely used to identify pollution  
154 sources and quantify their contributions to the ambient air pollutants at receptor sites, with an assumption of mass  
155 conservation between emission sources and receptors ([Amato et al., 2009](#); [Lee et al., 2008](#)). In this study, the United States  
156 Environmental Protection Agency (USEPA) PMF version 5.0 ([Norris et al., 2014](#)) was applied to perform the analysis.  
157 PMF decomposes the measured data matrix,  $X_{ij}$ , into a factor profile matrix,  $f_{kj}$ , and a factor contribution matrix,  $g_{ik}$ , (Eq  
158 3):

$$159 \quad x_{ij} = \sum_{k=1}^p g_{ik} f_{kj} + e_{ij} \quad (3)$$

$$160 \quad Q = \sum_{i=1}^n \sum_{j=1}^m (e_{ij}/u_{ij})^2 \quad (4)$$

161 where  $X_{ij}$  is the measured ambient concentration of target pollutants;  $g_{ik}$  is the source contribution of the  $k_{th}$  factor to  
162 the  $i_{th}$  sample, and  $f_{kj}$  is the factor profile of the  $j_{th}$  specie in the  $k_{th}$  factor;  $e_{ij}$  is the residual concentration for each data point.  
163 PMF seeks a solution that minimizes an object function  $Q$  (Eq 4), with the uncertainties of each observation ( $u_{ij}$ ) provided  
164 by the user.

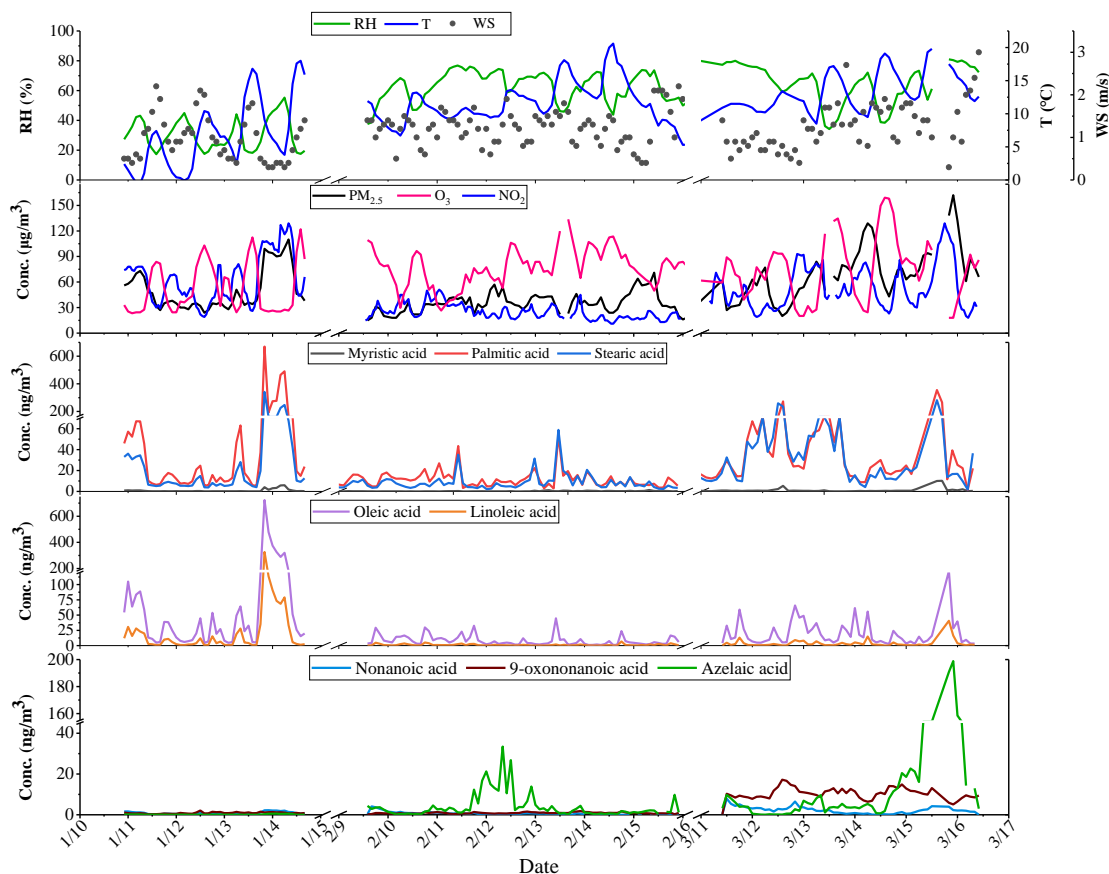
165 The uncertainty of each data point was calculated according to Eq 5:

$$166 \quad u_{ij} = \sqrt{(x_{ij} \times EF)^2 + (\frac{1}{2} \times MDL)^2} \quad (5)$$

167 where MDL is the method detection limit and  $EF$  is the error fraction determined by the user and associated with the  
168 measurement uncertainties. The concentration data below MDL was replaced by 0.5 of the MDL, and the corresponding  
169 uncertainty  $u_{ij}$  was calculated by five-sixths of the MDL. Missing values were replaced by the median value of the species,  
170 and its  $u_{ij}$  was assigned as four times of the median value ([Norris et al., 2014](#)).

## 171 3. Results and discussion

172 The time series of hourly data of meteorological parameters, gaseous pollutants (including O<sub>3</sub> and NO<sub>2</sub>), PM<sub>2.5</sub>, water  
173 soluble ions, carbon components during the monitoring period (January 10-14, February 9-15 and March 11-16, 2021) are  
174 shown in Fig.2. During the campaign, the average temperature (T), relative humidity (RH) and wind speed (WS) was 10.9  
175 ±4.5 °C, 55.3±18.2% and 1.2±0.5 m/s, respectively. The average concentrations of gas pollutants, PM<sub>2.5</sub>, water soluble  
176 ions and OC/EC are listed in Table S2. The average concentrations of NO<sub>2</sub>, O<sub>3</sub> and PM<sub>2.5</sub> were 42.85±25.89, 51.53±29.62  
177 and 50.07±26.54 µg/m<sup>3</sup>, respectively. Additionally, the average OC and EC concentrations were 6.57±4.63 and 2.12±2.04  
178 µg/m<sup>3</sup> respectively, with the contribution of OC to PM<sub>2.5</sub> ranging from 4.7% to 26.8% (13.2% as average).



179

180 **Figure 2.** Time series of pollutants concentration and meteorological parameters

181 **3.1 Characteristics of cooking-derived organic molecular markers**

182 The fatty acids studied include three most abundant sFAs (myristic, palmitic and stearic acids) and two abundant uFAs  
 183 (oleic and linoleic acids). The concentration of total fatty acids (TFAs, sum of the concentrations of the five fatty acids)  
 184 was  $(105.70 \pm 230.28)$   $\text{ng/m}^3$ , ranging from 8.30 to 2066.30  $\text{ng/m}^3$ , which is close to the concentrations at the urban site in  
 185 Shanghai ( $105 \text{ ng/m}^3$ ) (Li et al., 2020; Wang et al., 2020). The average percentage of TFAs in OC was 1.3% with the  
 186 maximum value of 8.7% (The concentration of  $\text{PM}_{2.5}$  at the corresponding time was  $99 \mu\text{g/m}^3$ ), which was 6.6 times higher  
 187 than the average. It revealed that the composition of  $\text{PM}_{2.5}$  could dramatically change, especially during the dinner time  
 188 (18:00-20:00). The mean concentration of TFAs at dinner time was  $172.89 \text{ ng/m}^3$ , and the contribution of TFAs to  $\text{PM}_{2.5}$   
 189 and OC mass concentration was 2.7‰ and 1.8%, respectively, which were 1.6 and 1.4 times of the mean during the  
 190 observation period.

191 We define the “polluted period” as the periods with hourly  $\text{PM}_{2.5}$  concentrations exceeding  $35 \mu\text{g/m}^3$ , and the  
 192 remaining periods are defined as “clean period”. Table 2 shows the mean values of  $\text{PM}_{2.5}$ , OC, TFAs concentrations and  
 193 meteorological conditions during the clean ( $\text{PM}_{2.5} < 35 \mu\text{g/m}^3$ ) and polluted periods ( $\text{PM}_{2.5} \geq 35 \mu\text{g/m}^3$ ). Generally, the



194 meteorological conditions during the polluted period are unfavourable compared to the clean period, showing lower wind  
 195 speed and higher humidity. The ratios of WS, T and RH during the polluted period to the clean period are 0.9, 1.0 and 1.1  
 196 respectively. The mean concentration of PM<sub>2.5</sub> during the polluted period was 62.86 µg/m<sup>3</sup>, which was 2.2 times higher  
 197 than that during the clean period (28.29 µg/m<sup>3</sup>). OC and PM<sub>2.5</sub> were similar, with concentrations during the pollution period  
 198 being 2.0 times higher than during the clean period. The mean concentration of TFAs in the polluted period was 147.06  
 199 ng/m<sup>3</sup>, 4.2 times higher than that in the clean hours (35.28 ng/m<sup>3</sup>). Additionally, the concentrations of sFAs and uFAs in  
 200 the polluted hours were 4.3 and 4.1 times higher than those during the clean period, respectively.

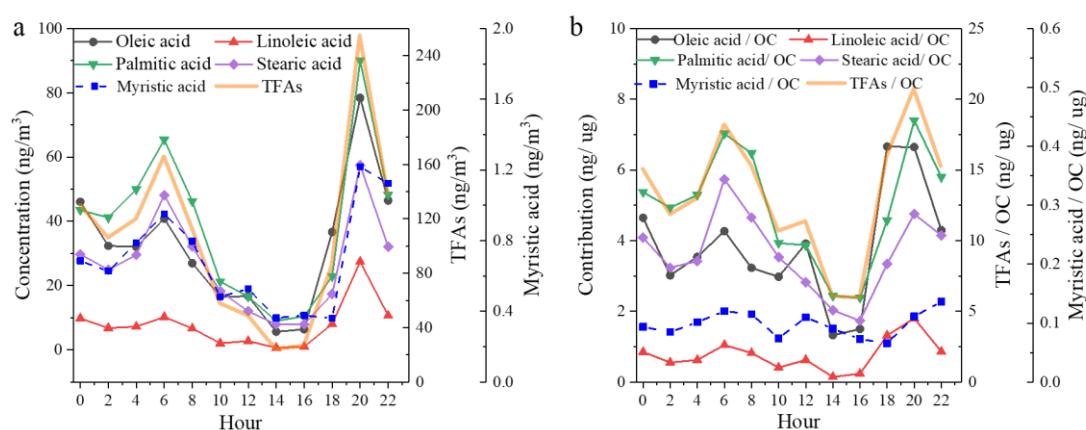
201 The concentration of TFAs were influenced by emissions, accumulation, transport and dispersion of pollutants during  
 202 the polluted periods (Hou et al., 2006; Schauer et al., 2003). The fatty acid content of 1.95 ng/µg in PM<sub>2.5</sub> during the  
 203 polluted period was 1.6 times greater than that of 1.24 ng/µg during the clean period, which was smaller than the variation  
 204 range of PM<sub>2.5</sub> and OC concentrations before and after the polluted period. The variation of TFAs in OC was similar to that  
 205 in PM<sub>2.5</sub>. Table S1 shows the contribution of total fatty acids directly emitted from various sources to OC, in which the  
 206 contribution of TFAs from vehicle exhaust is the least, and the proportion of TFAs emitted from cooking in OC is higher  
 207 than that from other sources. The change in TFAs/OC was weaker than the change in OC, mainly because cooking has  
 208 relatively small fluctuations in emissions, while the increase in OC concentration was more significant with simultaneous  
 209 contributions from other sources (e.g., biomass burning, coal combustion, and vehicle exhaust). Similarly, the mass  
 210 concentration of PM<sub>2.5</sub> was driven by emission source significantly. The observed contribution of TFAs to OC in PM<sub>2.5</sub> was  
 211 smaller than TFAs/OC ratio in cooking, but larger than that in other sources.

212 **Table 2. PM<sub>2.5</sub> concentration, organic carbon fraction, fatty acids concentration and meteorological conditions during clean**  
 213 **and polluted periods.**

Species	Clean period	Polluted period	Polluted/clean
PM <sub>2.5</sub> (µg/m <sup>3</sup> )	28.29 ± 5.27	62.86 ± 25.67	2.2
OC (µg/m <sup>3</sup> )	4.05 ± 1.09	8.00 ± 5.23	2.0
TFAs (ng/m <sup>3</sup> )	35.28 ± 28.17	147.06 ± 281.66	4.2
sFAs (ng/m <sup>3</sup> )	21.60 ± 14.91	92.05 ± 162.75	4.3
uFAs (ng/m <sup>3</sup> )	13.68 ± 14.22	55.53 ± 133.82	4.1
TFAs/PM <sub>2.5</sub> (ng/µg)	1.24 ± 0.91	1.95 ± 2.85	1.6
TFAs/OC (ng/µg)	9.52 ± 7.79	15.33 ± 14.59	1.6
WS (m/s)	1.23 ± 0.45	1.14 ± 0.54	0.9
T (°C)	10.77 ± 4.22	10.99 ± 4.68	1.0
RH (%)	53.41 ± 17.49	56.33 ± 18.55	1.1

214 Similar variation and diurnal patterns were found for these five fatty acids (Fig.3), confirming their common origin.  
 215 In addition, compared to fatty acids, the time series of C<sub>9</sub> acids showed a different diurnal variation, suggesting different

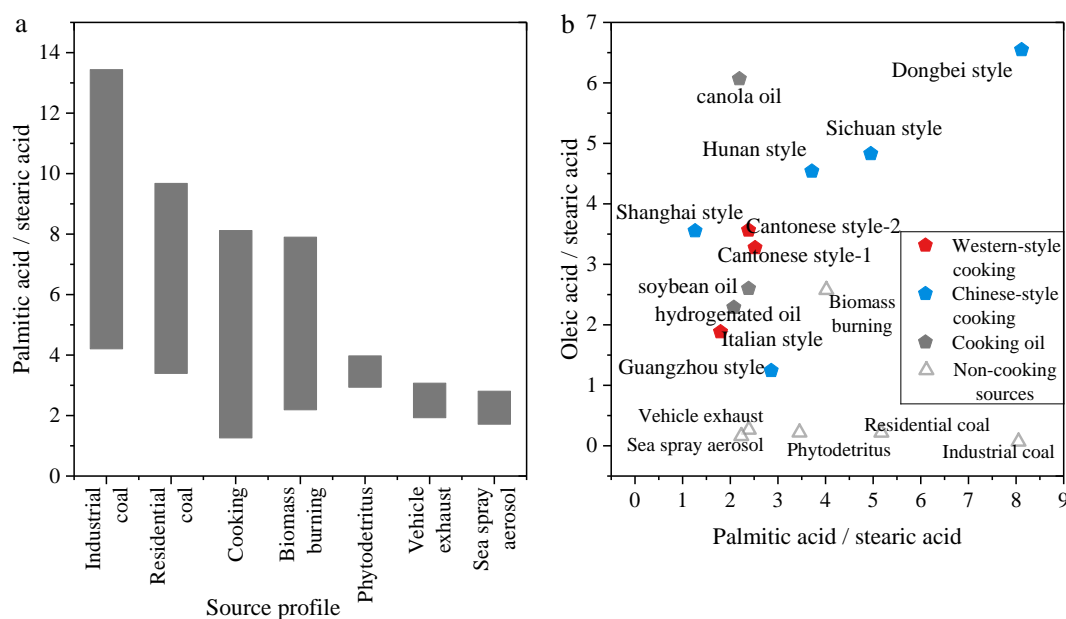
216 production and reaction processes. Fatty acids showed a clear diurnal variation, with two peaks observed at around 6:00  
 217 and 20:00 local time, respectively, and the dinner time peak was especially prominent. In contrast to the previous  
 218 observations in Shanghai, no peak was observed at lunchtime. The relatively higher boundary layer during the daytime,  
 219 facilitated the diffusion of pollutants. The weaker oxidation of uFAs emitted at night made the fatty acid concentration  
 220 peaks more pronounced at dinner time (Wang et al., 2020). Figure 3(b) shows the contribution of various fatty acids to OC.  
 221 From the diurnal patterns, it is shown that the proportion of the five fatty acids and TFAs in OC at noon had a weaker peak,  
 222 which was still smaller than that during the morning and evening mealtimes. In conclusion, the apparent peaks of TFAs at  
 223 the dinner time provide evidence for major source contribution to air pollution from local cooking emissions, although  
 224 there are mix sources including vehicle exhaust, coal combustion, etc.



225  
 226 **Figure 3. Diurnal variation of five fatty acids and TFAs during the observation period.**

227 Fatty acids in urban atmospheres are influenced by various anthropogenic (e.g., biomass burning, vehicle exhaust)  
 228 (Hays et al., 2002; Schauer et al., 2001; Simoneit, 2002; Wang et al., 2009) and biogenic sources (Oliveira et al., 2007;  
 229 Rogge et al., 2006). The main sources of fatty acid-like substances in the ambient air of the study area can be discerned on  
 230 the basis of characteristic ratios between fatty acids emitted from different sources (Fig.4) (He et al., 2004; Pei et al., 2016;  
 231 Rogge et al., 1993; Zhao et al., 2015; Zhao et al., 2007). The palmitic acid to stearic acid (P/S) ratios observed in this study  
 232 ranges between 0.49 and 3.08 (average value: 1.49), significantly lower than those associated with residential coal  
 233 combustion and industrial coal combustion, while partially overlapping those from biomass burning, vehicle exhaust and  
 234 sea spray aerosol (Bikkin et al., 2019; Cai et al., 2017; Ho et al., 2015; Zhang et al., 2008; Zhang et al., 2007). Ho et al.  
 235 (2015) investigated urban areas in Beijing where fatty acid concentrations were elevated during traffic restrictions  
 236 compared to non-restricted periods, suggesting that motor vehicle exhaust is not the largest source of fatty acids in urban  
 237 areas. The information on fatty acid emissions from biomass burning source is closer to that of cooking sources (Hays et

238 [al., 2002](#); [Schauer et al., 2001](#); [Zhang et al., 2008](#)), however, in the study of [Simoneit \(2002\)](#), no oleic acid was detected in  
 239 organic molecular substances from biomass burning. The oleic acid/stearic acid (O/S) ratio from sea spray aerosol samples  
 240 is 0.16 ([Bikkin et al., 2019](#)), which is obviously lower than the ambient data in this study (1.4). Hence, during the  
 241 observation in this study, vehicle exhaust and sea spray were not the most important sources of fatty acids emissions in  
 242 urban Changzhou. Especially during the dinner period, when the O/S ratio was significantly higher and close to the ratio  
 243 in the organics emitted from traditional culinary types in the Yangtze River Delta region.

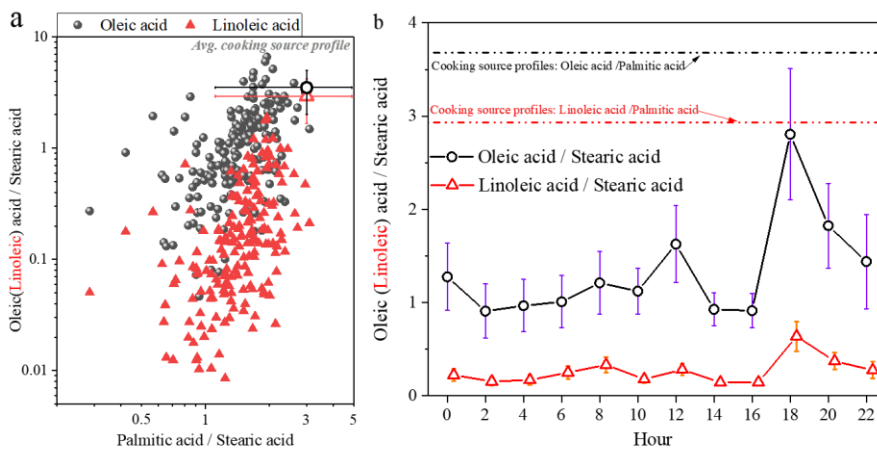


244 **Figure 4. Ratio of fatty acids (P/S) in organic molecular substances emitted directly from different sources (a); Ratio of fatty**  
 245 **acids (P/S vs O/S) emitted by different types of cooking sources and non-cooking sources (b).** ([Bikkin et al., 2019](#); [Cai et al.,](#)  
 246 [2017](#); [Hays et al., 2002](#); [He et al., 2004](#); [Oliveira et al., 2007](#); [Pei et al., 2016](#); [Rogge et al., 1993](#); [Schauer et al., 2001](#); [2002](#);  
 247 [Simoneit, 2002](#); [Zhang et al., 2008](#); [Zhao et al., 2007](#)).

249 Information on the changes of specific molecular markers is useful in investigating the aging process of aerosol. The  
 250 two uFAs (oleic acid and linoleic acid) are more reactive with atmospheric oxidants (OH and O<sub>3</sub>, etc.) in the atmosphere  
 251 due to the presence of C=C bonds, compared to sFAs. Furthermore, the two homologous sFAs (palmitic and stearic acid)  
 252 have similar chemical structures, reactivity and volatility, thus their concentration ratios can be assumed to remain constant  
 253 during post-emission periods. Therefore, the ratio of P/S mainly depends on the sources. [Fig.5 shows the O/S ratios and](#)  
 254 [linoleic acid/ stearic acid \(L/S\) versus P/S, respectively.](#) The average value of P/S was 1.49±0.49, which was within the  
 255 [range of cooking source profile values measured from direct emissions from different restaurants and cooking types \(1.3-](#)  
 256 [8.1\) \(He et al., 2004; Pei et al., 2016; Schauer et al., 2002; Zhao et al., 2007\), and similar to the ratio of P/S in atmospheric](#)  
 257 [PM<sub>2.5</sub> in Shanghai \(1.9\) \(Li et al., 2020; Wang et al., 2020\).](#) In this study, the O/S ratio (1.4 ± 1.1) of the ambient samples  
 258 [was overall in the range of the cooking source profile \(3.6 ± 1.6\), while the L/S ratio of 0.25 ± 0.31 was slightly lower than](#)

259 the cooking source profile values ( $2.9 \pm 1.8$ ) (He et al., 2004; Pei et al., 2016; Schauer et al., 2002; Zhao et al., 2007). The  
 260 results of Moise and Rudich (2002) showed that the reactant activity is directly related to the concentration of unsaturated  
 261 bonds, with linoleic acid having an extra double bond than oleic acid, indicating that linoleic acid is more easily degraded  
 262 than oleic acid (Moise and Rudich, 2002; Thornberry and Abbatt, 2004). The O/S ratio of the ambient samples in this study  
 263 was higher than those measured in Beijing (0.65) (He et al., 2004) from January to October and in Shanghai (0.83) (Li et  
 264 al., 2020; Wang et al., 2020) during winter.

265 The diurnal variations of O/S and L/S are also shown in Fig.5. The ratios were significantly higher during dinner time,  
 266 and were closer to the cooking source profile. Demonstrating that changes in fatty acid concentrations may be influenced  
 267 primarily by cooking source emissions, especially during dinner time when fresh cooking source emissions entered into  
 268 the atmosphere and uFAs were quickly consumed due to aging. The ratio of linoleic acid to stearic acid is consistently  
 269 lower than what is involved in the source spectrum, which may be influenced by different regions and source characteristics  
 270 from different types of restaurants, as well as small emissions from other minor sources.



271  
 272 **Figure 5. The oleic/ stearic acid and linoleic/ stearic acid ratios compared to the palmitic/stearic acid ratio (a); diurnal variation**  
 273 **in the ratio of oleic (linoleic) acid to stearic acid concentration (b). (The cooking source profile values were measured from direct**  
 274 **emissions from different restaurants and cooking types.) (He et al., 2004; Pei et al., 2016; Schauer et al., 2002; Zhao et al., 2007).**

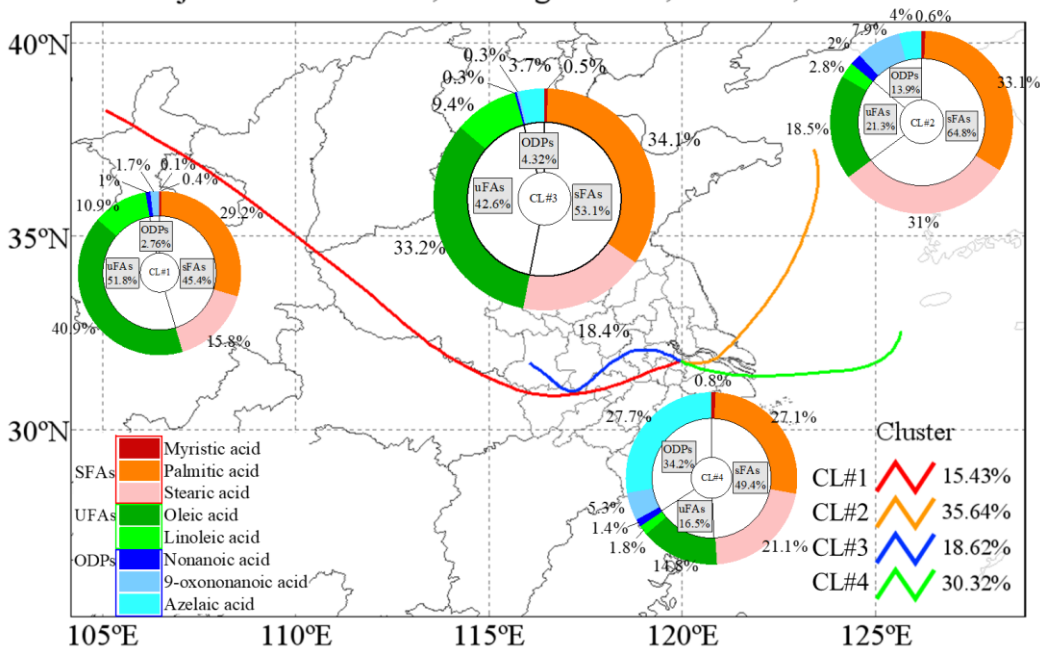
### 275 3.2 Backward trajectory clustering analysis

276 The best solution of four clusters was determined based on the variation of the total spatial variance (Fig.6 and Fig.  
 277 S2). Fig.7 shows the four cluster solutions and the mean distribution of meteorological conditions and pollutants in each  
 278 cluster. Briefly, cluster #1 (CL#1), which represents 15.4% of the sample, comes from the northwest continental region of  
 279 China and reaches Changzhou before passing Gansu, Shan'xi and Henan provinces, and the lower temperature and  
 280 humidity associated with this cluster are consistent with its geographic origin. Cluster #2 (CL#2), which accounts for 35.6%  
 281 of the total number of trajectories, represents air masses from the northeastern part of the ocean, and the temperature and

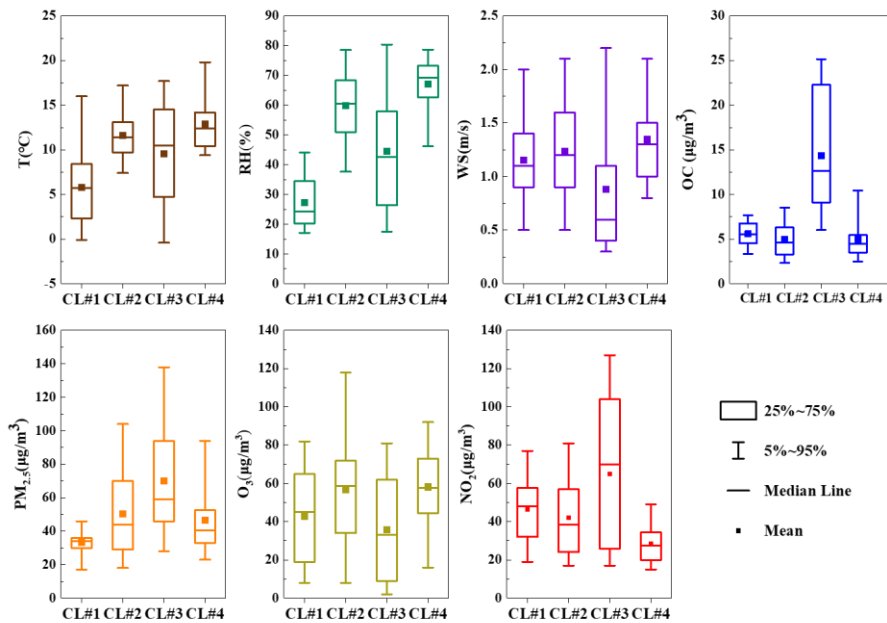
282 humidity associated with this cluster are higher than those of CL#1. Cluster 3 (CL#3), contributing 18.6%, traveling slowly  
283 from inland area, is associated with the lowest wind speed, with higher temperature and humidity than CL#1 but lower  
284 than CL#2. Cluster 4 (CL#4), representing 30.3% of the trajectories, represents the eastern/southeastern oceanic air masses,  
285 with the highest observed temperature, humidity and wind speed among all of the air masses. CL#2 and CL#4 have  
286 relatively high temperature, humidity and wind speed. CL#3 is associated with the highest NO<sub>2</sub> concentrations, confirming  
287 its local air mass origin, and the PM<sub>2.5</sub> and OC concentrations in this air mass are also the highest compared to all the other  
288 air masses.

289 **The concentrations of sFAs, uFAs and their oxidation products under each cluster are shown in Fig.6.** The total  
290 concentrations of sFAs, uFAs and uFAs' oxidative decomposition products (ODPs, in this study, ODPs includes azelaic  
291 acid, nonanoic acid and 9-oxononanoic acid) within the four types of air mass clusters were in the order of  
292 CL#3>CL#2>CL#4>CL#1, where the TFAs in CL#1 and CL#3 were larger than the percentages in CL#2 and CL#4. The  
293 relative contents of sFAs and uFAs in CL#1 and CL#3 are closer than those in the other two types of air masses, and are  
294 closer to the concentration ratio of the species directly emitted from the cooking source (the value of uFAs /sFAs range  
295 from 0.8 to 3.2) ([He et al., 2004](#); [Pei et al., 2016](#); [Schauer et al., 2002](#); [Zhao et al., 2007](#)), which indicated that the oxidative  
296 decomposition of uFAs is less in CL#1 and CL#3. CL#3 was a slowly moving, local cluster. Under this air mass clustering,  
297 local emissions contribute significantly to fatty acids as well as PM<sub>2.5</sub> concentration. The air mass of CL#1 exhibits the  
298 longest range, the concentrations of ODPs were relatively small among all air masses, and the low ODPs concentration  
299 was inconsistent with other literature findings of more aging aerosol production from long-range transport ([Wang et al.,](#)  
300 [2020](#)). The lowest PM<sub>2.5</sub> concentrations and cleaner air masses during air mass CL#1 suggested that long-range air mass  
301 transport from the northwest was not the main source of fatty acids and ODPs in Changzhou during the observation. The  
302 value of uFAs /sFAs in CL#2 and CL#4 was less than that in CL#1 and CL#3 and less than the ratio in sources. In addition,  
303 the proportion of ODPs in CL#2 and CL#4 is greater than that in CL#1 and CL#3. This result may be explained by the  
304 following two reasons: first, under the influence of transport, the air masses brought more sFAs, ODPs, and the air masses  
305 were more aged, **for example, marine heterotrophic bacteria releases sFAs and uFAs into the water column, however the**  
306 **mono/polyunsaturated fatty acids (e.g., oleic acid, linoleic acid) in seawater rapidly oxidizes to form initially oxocarboxylic**  
307 **acids, azelaic acid etc. ([Bikkin et al., 2019](#));** second, under the influence of CL#2 and CL#4 air masses, in which the ozone  
308 concentration was higher than other air masses, the decomposition reaction of uFAs was more active and could produce  
309 more ODPs. In addition, the oxidative reaction of uFAs could be influenced by meteorological conditions as well.

TrajStat-Cluster means, arriving at 100m, 31.46°N, 119.96°E



310  
311 **Figure 6. Sources for each air mass during the sampling period. The colored lines in the map show the contribution of each**  
312 **directional air mass source to the total trajectory as resolved by the TrajStat model.**

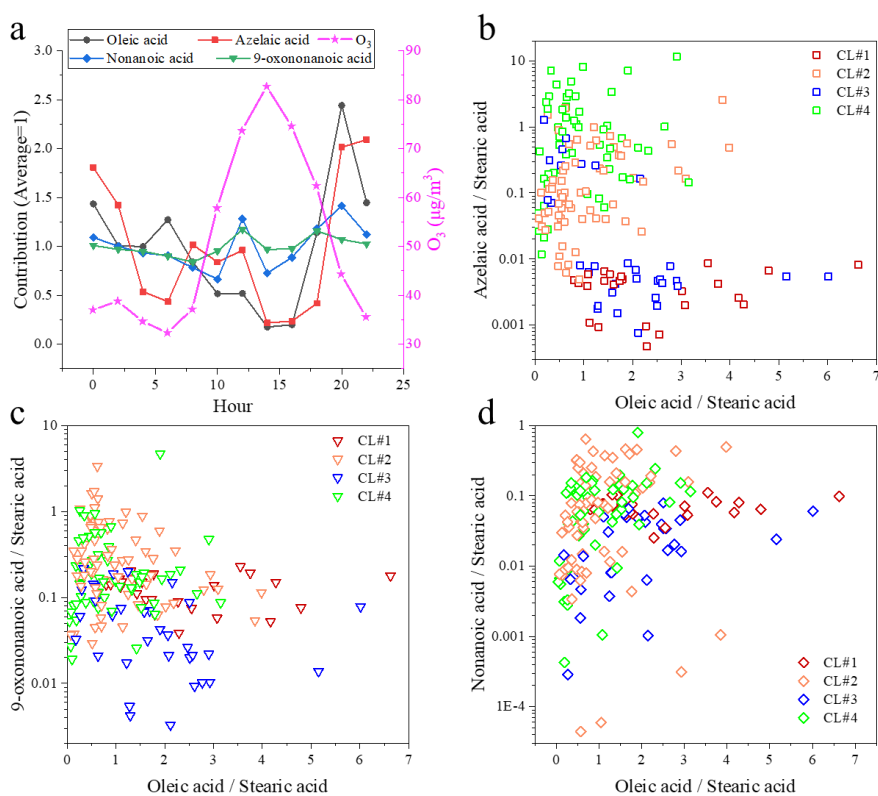


313  
314 **Figure 7. Box plots of meteorological parameters and pollutant concentrations in each cluster (squares and solid lines**  
315 **correspond to the mean and median, respectively; boxes indicate the 25<sup>th</sup> and 75<sup>th</sup> percentiles, whiskers are the 5<sup>th</sup> and 95<sup>th</sup>**  
316 **percentiles).**

### 317 **3.3 Atmospheric aging of unsaturated fatty acids**

318 Fig.8(a) shows the diurnal variation of ozone, oleic acid, and ODPs. The ozone concentration started to rise in the  
319 morning (06:00) and peaked in the late afternoon (14:00). The diurnal trend of oleic acid was opposite to that of ozone.  
320 The diurnal trend of ODPs was also different from oleic acid, the small peak of ODPs was found at around 12:00 in the

321 daytime, which was earlier than that of ozone. At the same time, oxidative decomposition, atmospheric dilution and lower  
 322 emissions caused significant decrease in the concentration of oleic acid until night when large amounts of fresh emissions  
 323 enter the atmosphere again. The decreasing rate of oleic acid concentration slowed down around noon, probably because  
 324 of fresh emission (e.g., cooking source) at lunch time. C9  $\omega$ -oxo acid and diacids (e.g., nonanoic acid, 9-oxononanoic acid  
 325 and azelaic acid) in the atmospheric environment originate from plant volatilization, combustion emissions, and cooking  
 326 processes (Kawamura et al., 2013; Tian et al., 2020), and they were established in chamber studies as major atmospheric  
 327 oxidation products from uFAs ozonolysis (Kawamura et al., 2013; Moise and Rudich, 2002; Thornberry and Abbatt, 2004).  
 328 The diurnal variations of Nonanoic acid and 9-oxononanoic acid were similar and both peaked around noon, while the  
 329 production of 9-oxononanoic acid and azelaic acid are in competition (Thornberry and Abbatt, 2004). However, the  
 330 concentration of 9-oxononanoic acid was significantly higher than that of nonanoic acid (Fig.8, c and d), which may be  
 331 due to the following reasons: (1) 9-oxononanoic acid can be produced by two pathways, while nonanoic acid generation  
 332 can only be produced through one of the pathways competing with nonanal, and the molarity generated from the ozonolysis  
 333 of oleic acid is smaller than that of 9-oxononanoic acid (Gross et al., 2009); (2) due to the high volatility of nonanoic acid,  
 334 its concentration in the particle phase is much lower, and only a small portion of nonanoic acid in PM is detected by TAG  
 335 (Wang and Yu, 2021).



336  
 337 **Figure 8. Diurnal variation of C9 products and oleic acid in environmental samples compared to O<sub>3</sub> (a); Correlation of C9**

338 **products azelaic acid (b), 9-oxononanoic acid (c), and nonanoic acid (d) with oleic acid.**

339 Fig.8(b) to (d) show the relationship between ODPs / stearic acid ratio and oleic acid/stearic acid. In CL#2 and CL#4,  
340 9-oxononanoic acid / stearic acid ratio is larger than that in CL#1 and CL#3, and azelaic acid /stearic acid ratio have the  
341 same characteristic. The nonanoic acid / stearic acid ratio is not well characterized, probably because most of the nonanoic  
342 acid is present in the gas phase. Bikkina et al. (2019) found that the O/S ratio exhibited a nonlinear (power) inverse  
343 relationship with azelaic acid in remote marine aerosols. This feature was not found in this study, which is possibly due to  
344 the single source class of fatty acids and ODPs in remote marine areas, the diversity of emission sources in urban areas,  
345 and their vulnerability to transport.

### 346 **3.4 Oxidative decomposition of uFAs**

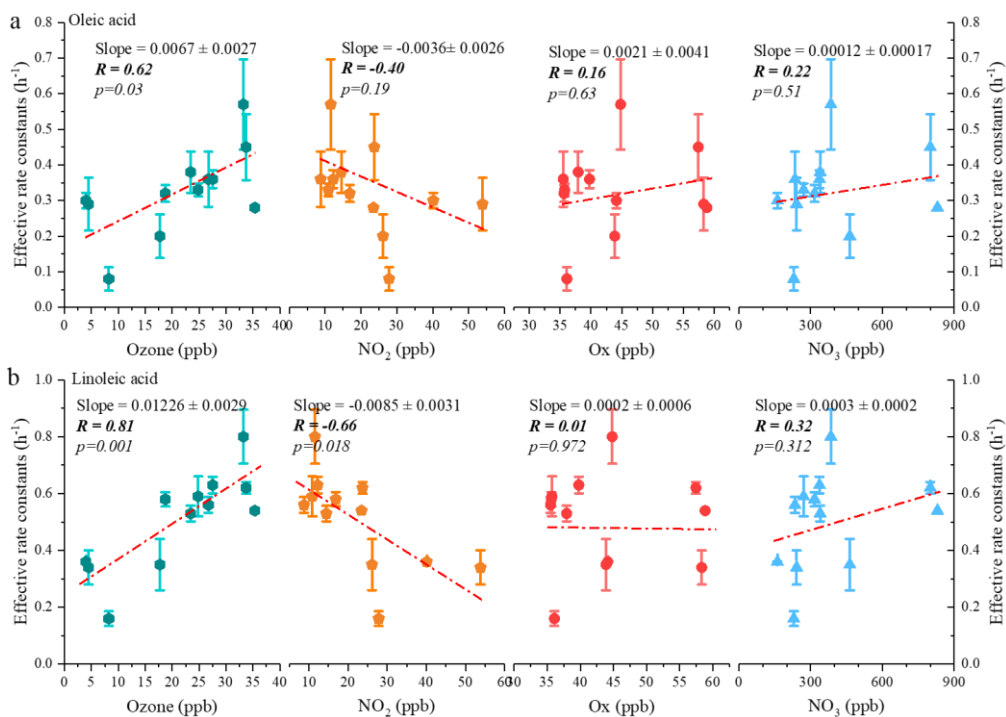
347 From the above analysis, cooking emission was the most important source of fatty acids in atmospheric PM<sub>2.5</sub> in urban  
348 areas of Changzhou, especially during the dinner period. Both sFAs and uFAs peaked between 18:00 and 22:00 pm, and  
349 then declined until breakfast time in the next day. Fatty acid-like substances in fresh cooking emissions react with various  
350 oxidants while being continuously replenished by the fresh cooking emission during the day so that the degradation of  
351 uFAs in the particulate phase can be complicated. With no obvious fresh cooking emissions after dinner, and the low  
352 volatility of the target pollutants studied (oleic and linoleic acids), the effect of gas-particle partitioning on them can be  
353 disregarded, and the evening provides a good opportunity to investigate the chemical degradation of uFAs from cooking  
354 emissions. Therefore, we selected the period from 18:00 in the evening to 6:00 in the morning, focusing on the impact of  
355 oxidants in the atmospheric environment on uFAs. The definition of the effective rate constant  $k$  has been described in  
356 previous studies (Donahue et al., 2005; Wang and Yu, 2021). To calculate the rate constant of uFAs with oxidants (especially  
357 O<sub>3</sub> and NO<sub>3</sub><sup>\*</sup>, etc), a one-step model was utilized, and an average decay rate constant at each night could be derived. The  
358 same method has been used in the study of Wang and Yu (2021), which shows that more than 77% of the observed data fits  
359 better with a one-step model. Figures S5 and S6 show the night-time oxidative degradation of oleic acid and linoleic acid,  
360 respectively. It should be noted that not all of the reactants (uFAs) will be fully consumed from the start of the fit until fresh  
361 emissions enter the atmosphere, and the amount of consumed and remaining uFAs could be affected by a combination of  
362 oxidant level, source activity, and meteorological conditions.

363 Fig.9 shows the effective rate constants of the oxidative decomposition of oleic ( $k_O$ ) and linoleic ( $k_L$ ) acids in relation  
364 to air oxidants (O<sub>3</sub>, NO<sub>2</sub>, O<sub>x</sub> and NO<sub>3</sub><sup>\*</sup>, etc. O<sub>x</sub> is the total oxidant, calculated from O<sub>x</sub> = NO<sub>2</sub> + O<sub>3</sub>). It should be noted that  
365 the NO<sub>3</sub><sup>\*</sup>, calculated by multiplying O<sub>3</sub> by NO<sub>2</sub>, is a substitution for NO<sub>3</sub><sup>\*</sup> radical, which is not available in this campaign.

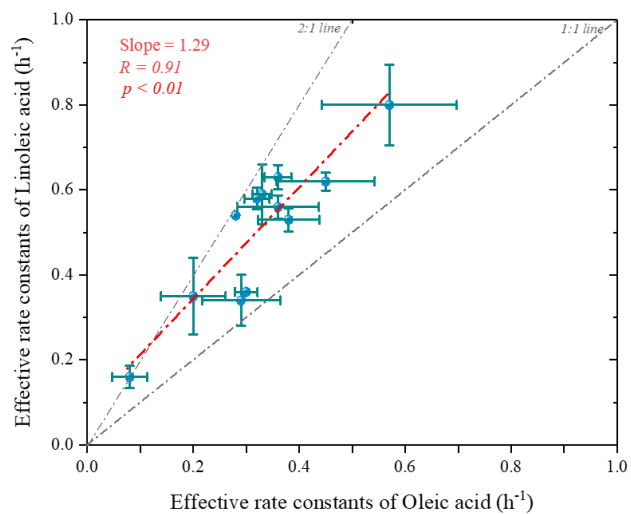


366 Both  $k_O$  and  $k_L$  had a significant positive correlation (The P values of significance tests were all less than 0.05) with  $O_3$ ,  
367 and no correlation was observed with other air oxidants ( $O_3$ ,  $NO_3^*$  and  $NO_2$ ). Ozone acted as the predominant oxidant for  
368 the oxidative decomposition of uFAs, which was consistent with the conclusion in Shanghai. In addition to the oxidants  
369 mentioned above, laboratory studies has also reported  $N_2O_5$  reacts with olefinic acids containing C=C bonds such as oleic  
370 acid and linoleic acid, which has a much slower reaction kinetics than that of  $NO_3^*$  (Gross et al., 2009). Therefore, the  
371 effect of  $N_2O_5$  was ignored in this study.

372 Fig.10 shows the scatter plot of the effective rate constants of oleic and linoleic acid. The significant correlation  
373 between the effective rate constants of oleic acid and linoleic acid was not equal to 1 due to the differences in aerosol  
374 composition and environmental conditions. The effective rate constant of oleic acid ranged from 0.08-0.57  $h^{-1}$ , which was  
375 overall smaller than  $k_L$  (0.16-0.80  $h^{-1}$ ), indicating that their reactivity is closely related to their chemical structure, and the  
376 two -C=C- bonds in the linoleic make a higher probability in reacting with atmospheric oxidants. However, besides the  
377 chemical structure, other factors (e.g., diffusion, and temperature) also affect the calculation of oxidation reaction rate of  
378 uFAs. The fitted ratio of  $k_L/k_O$  is 1.29 (red dashed line in Fig.11), with most scatters fall in the area with  $k_L$  to  $k_O$  values  
379 above the 1:1.  $k_L/k_O$  has a mean value of  $1.6 \pm 0.3$  and the relative reactivity of linoleic acid to oleic acid is below 2 in the  
380 measured environmental data, but close to the results of laboratory studies with  $O_3$  as oxidant. We also reviewed the  $k_L/k_O$   
381 ratios of  $O_3$ ,  $NO_3^*$  and  $N_2O_5$  as oxidants in other laboratory studies, and the  $k_L/k_O$  ratios of the three oxidants were 1.7, 1.8  
382 and 2.9 (Gross et al., 2009; Thornberry and Abbatt, 2004), respectively. The relative reaction coefficients  $k_L/k_O$  measured  
383 for  $O_3$  in laboratory studies are close to our results. The comparison indicates that  $O_3$  was the most likely oxidants for the  
384 nighttime uFAs oxidation in the urban area of Changzhou.



385  
 386 **Figure 9. Correlations of the estimated effective decay rate constant with average night-time atmospheric oxidants**  
 387 **concentration for oleic acid (a) and linoleic acid (b). (The p-value indicates the parameter of the F-test of the regression**  
 388 **equation in the regression model.)**



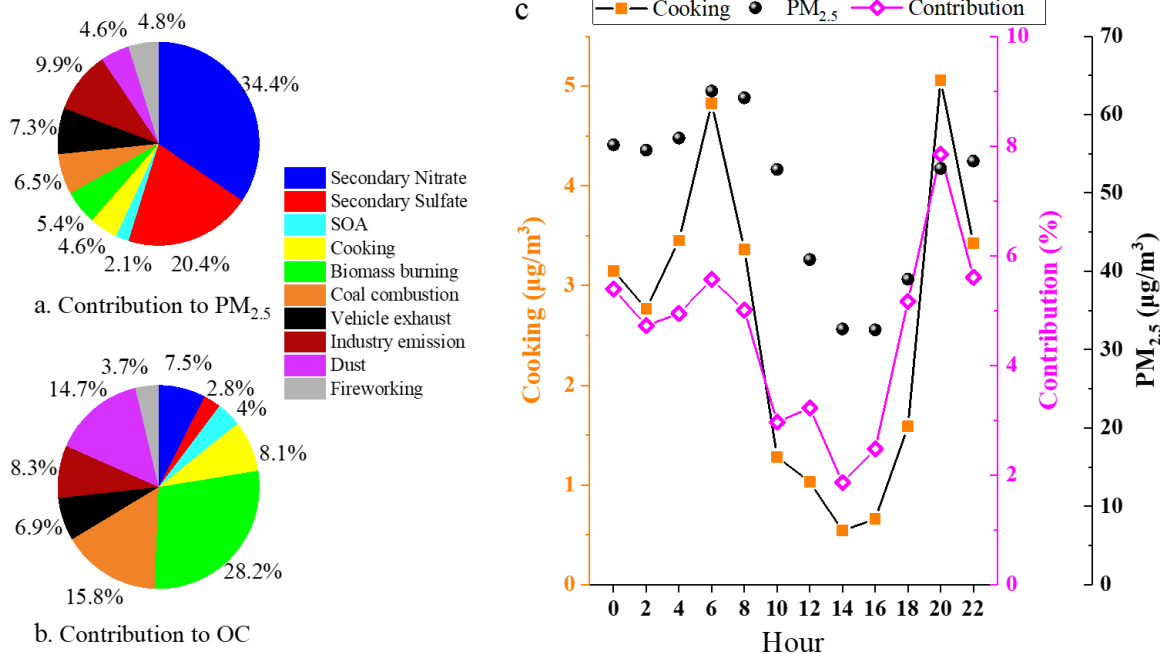
389  
 390 **Figure 10. Scatter plot of the estimated effective rate constant for linoleic acid versus oleic acid (The p-value indicates the**  
 391 **parameter of the F-test of the regression equation in the regression model).**

### 392 3.5 Source contributions of cooking aerosol to PM<sub>2.5</sub> and OC

393 To gain a more quantitative assessment of source contribution from cooking to OA, PMF was applied for source  
 394 apportionment. The target POA markers were incorporated into the input data matrix, along with SOA markers (Table S1)  
 395 and major aerosol components including major ions, elements, EC, and OC. Source apportionment of PM<sub>2.5</sub> in this field

396 campaign yielded 10 sources, including three secondary sources (secondary sulfate, secondary nitrate and SOA,  
397 respectively) and seven primary emission sources (cooking, biomass burning, coal combustion, vehicle exhaust, industrial  
398 emissions, dust and fire working, respectively). A detailed description of the identification of each PMF-resolved source  
399 factor is shown in section S1. Briefly, secondary source factors account for the largest share of PM<sub>2.5</sub> (the total was 56.9%,  
400 of which secondary nitrate contributes up to 34.4%), and primary emissions contributed to 43.1% of total PM<sub>2.5</sub> (Fig.11).  
401 Among the primary source factors, industry makes the largest contribution to PM<sub>2.5</sub> mass concentration (9.9%).

402 In a specific pollution period, different sources have different impacts on PM<sub>2.5</sub> concentration and chemical  
403 compositions in Changzhou. Among the 10 sources, the cooking factor was dominated by sFAs and uFAs during the  
404 monitoring period, accounting for 4.6% of the total PM<sub>2.5</sub>. The concentration of cooking source and its contribution to total  
405 PM<sub>2.5</sub> also showed a clear diurnal variation, with two peaks at around 6:00 and 20:00, respectively, especially at the dinner  
406 time. The contribution of cooking to PM<sub>2.5</sub> concentration during mealtime increased significantly compared with other  
407 periods, reaching 7.8% at 20:00. The mean concentration of cooking aerosol in the polluted period was estimated to be 4.0  
408  $\mu\text{g}/\text{m}^3$ , which was 5.3 times higher than that in the clean period (0.75  $\mu\text{g}/\text{m}^3$ ). The variation was similar to that of fatty  
409 acids. The factor profiles of the 10-factor constrained run of PMF are shown in section S1 and Figure S5, together with the  
410 time series of contributions from individual source factors. Overall, we estimated that cooking accounted for 5.8% of the  
411 total PM<sub>2.5</sub> during the pollution period, which was 1.9 times greater than that of 3.0% during the clean period. During the  
412 whole observation period, the cooking factor contributes only a small part of PM<sub>2.5</sub> (4.6%), but it accounts for 8.1% of the  
413 total OC, indicating the importance of cooking emissions to organic matter, which is a significant source of organic  
414 pollution in urban areas.



415

416

**Figure 11. Comparison of individual factor contributions to PM<sub>2.5</sub> (a) and OC (b); diurnal variation of cooking source (c).**

417

#### 4. Conclusions

418

In this study, we measured uFAs, sFAs, and ODPs every two hours using TAG in the urban Changzhou city. The concentration of TFAs averaged at 105.70 ng/m<sup>3</sup>, close to that in Shanghai. The average concentration of TFAs in polluted period was 147.06 ng/m<sup>3</sup>, which was 4.2 times higher than that during clean period. During the rising period of PM<sub>2.5</sub>, TFAs concentration tends to reach the peak earlier than PM<sub>2.5</sub>, and the proportion of TFAs in PM<sub>2.5</sub> as well as OC will increase first and then decrease. However, when affected by adverse diffusion, TFAs concentration will accumulate continuously as PM<sub>2.5</sub>. The linoleic acid /stearic acid and oleic acid /stearic acid ratios exhibited a significant peak during dinner time, which was close to the cooking source profile values, and a relatively smaller peak at lunchtime. Cooking sources during dinner hours are the most important contributors to the concentration of fatty acids in PM<sub>2.5</sub> during the study period. Diurnal trend of ODPs was different from that of uFAs, and the concentration of ODPs increased significantly at noon. The diurnal variations of nonanoic acid and 9-oxononanoic acid in ODPs are similar, mainly because oleic acid can produce both 9-oxononanoic acid and nonanoic acid in the ozonolysis pathway.

429

Under the influence of different air masses, there were significant variations in the ratios of various organic acids from cooking. Highest total concentrations of sFAs, uFAs and ODPs were found under the local air mass cluster (CL#3), indicating significant local emissions contributing to fatty acids as well as PM<sub>2.5</sub>. And the percentages of TFAs in CL#1 and CL#3 were larger than that in CL#2 and CL#4. The proportion of ODPs in CL#2 and CL#4 was greater than that in CL#1 and CL#3. This is mainly because under the influence of transportation, the air masses brought more sFAs, ODPs.

433

434 The air masses were more aged, and the higher ozone concentration and more active uFAs decomposition reaction occurred  
435 in these two air mass clusters. The daily oxidative degradation kinetics of oleic and linoleic acids were obtained using data  
436 during night time of each observation date. The  $k_O$  ranged from 0.08 to 0.57 h<sup>-1</sup>, which was overall smaller than  $k_L$  (0.16-  
437 0.80 h<sup>-1</sup>). It was observed that both  $k_O$  and  $k_L$  had a significant positive correlation with O<sub>3</sub>. The relative reaction coefficients  
438  $k_L/k_O$  (1.6 ±0.3) of linoleic and oleic acids in this study are close to  $k_L/k_O$  measured for O<sub>3</sub> in laboratory studies, indicating  
439 that O<sub>3</sub> was the main night-time oxidants for uFAs in Changzhou City. Overall, this study describes the concentration  
440 variation and oxidative degradation of uFAs and oxidation products in ambient air based on hourly time-resolved  
441 observations, guiding future refinement of source apportionment of PM<sub>2.5</sub> and the development of cooking emission control  
442 policies.

443 The average contribution of cooking to PM<sub>2.5</sub> was estimated to be 4.6%, while the average contribution to total OC  
444 was 8.1%. However, the proportion of cooking to total PM<sub>2.5</sub> among different sources during the meal period increased  
445 significantly compared with other periods, especially during the dinner period, peaking at 7.8%. It is estimated that cooking  
446 source accounted for 5.8% of the total PM<sub>2.5</sub> during the pollution period, which was 1.9 times greater than the 3.0% during  
447 the clean period, showing that strict control on cooking emissions should be paid more attention during pollution episodes.

448

#### 449 **ACKNOWLEDGEMENTS**

450 This study is financially supported by the National Natural Science Foundation of China (NO. 41875161, 42075144 and  
451 42005112). We thank Changzhou Environmental Monitoring Center of Jiangsu Province to help conduct the field  
452 campaign.

#### 453 **AUTHOR CONTRIBUTIONS**

454 RL, KZ, QL and LMY conducted the field measurements. RL and KZ performed the data analysis and prepared the  
455 manuscript with contributions from all co-authors. LL formulated the research goals and edited and reviewed the  
456 manuscript. LL and JZY reviewed and edited the manuscript. All authors contributed to data interpretations and discussions.

#### 457 **COMPETING INTERESTS**

458 The authors declare no conflict of interest.

#### 459 **DATA AND CODE AVAILABILITY**

460 This paper does not report original code. Data is available from the corresponding author (Lily@shu.edu.cn) upon request.

#### 461 **REFERENCES**

462 Amato, F., Pandolfi, M., Escrig, A., Querol, X., Alastuey, A., Pey, J., Perez, N., and Hopke, P. K.: Quantifying road  
463 dust resuspension in urban environment by Multilinear Engine: A comparison with PMF2, *Atmos. Environ.*, 43(17), 2770-  
464 2780, doi:10.1016/j.atmosenv.2009.02.039, 2009.

465 Bertrand, A., Stefenelli, G., Jen, C. N., Pieber, S. M., Bruns, E. A., Ni, H. Y., Temime-Roussel, B., Slowik, J. G.,  
466 Goldstein, A. H., El Haddad, I., Baltensperger, U., Prevot, A. S. H., Wortham, H., and Marchand, N.: Evolution of the  
467 chemical fingerprint of biomass burning organic aerosol during aging, *Atmos Chem Phys*, 18(10), 7607-7624,  
468 doi:10.5194/acp-18-7607-2018, 2018a.

469 Bertrand, A., Stefenelli, G., Pieber, S. M., Bruns, E. A., Temime-Roussel, B., Slowik, J. G., Wortham, H., Prevot, A.  
470 S. H., El Haddad, I., and Marchand, N.: Influence of the vapor wall loss on the degradation rate constants in chamber  
471 experiments of levoglucosan and other biomass burning markers, *Atmos Chem Phys*, 18(15), 10915-10930,  
472 doi:10.5194/acp-18-10915-2018, 2018b.

473 Bikkin, P., Kawamura, K., Bikkina, S., Kunwar, B., Tanaka, K., and Suzuki, K.: Hydroxy Fatty Acids in Remote  
474 Marine Aerosols over the Pacific Ocean: Impact of Biological Activity and Wind Speed, *Acs Earth Space Chem*, 3(3), 366-  
475 379, doi:10.1021/acsearthspacechem.8b00161, 2019.

476 Cai, T. Q., Zhang, Y., Fang, D. Q., Shang, J., Zhang, Y. X., and Zhang, Y. H.: Chinese vehicle emissions characteristic  
477 testing with small sample size: Results and comparison, *Atmos Pollut Res*, 8(1), 154-163, doi:10.1016/j.apr.2016.08.007,  
478 2017.

479 Donahue, N. M., Robinson, A. L., Huff Hartz, K. E., Sage, A. M., and Weitkamp, E. A.: Competitive oxidation in  
480 atmospheric aerosols: The case for relative kinetics, *Geophys. Res. Lett.*, 32(16), doi:10.1029/2005gl022893, 2005.

481 Fortenberry, C., Walker, M., Dang, A., Loka, A., Date, G., de Carylho, K. C., Morrison, G., and Williams, B.: Analysis  
482 of indoor particles and gases and their evolution with natural ventilation, *Indoor Air*, 29(5), 761-779, doi:10.1111/ina.12584,  
483 2019.

484 Gross, S., Iannone, R., Xiao, S., and Bertram, A. K.: Reactive uptake studies of NO<sub>3</sub> and N<sub>2</sub>O<sub>5</sub> on alkenoic acid,  
485 alkanolate, and polyalcohol substrates to probe nighttime aerosol chemistry, *PCCP*, 11(36), 7792-7803,  
486 doi:10.1039/b904741g, 2009.

487 Hays, M. D., Geron, C. D., Linna, K. J., Smith, N. D., and Schauer, J. J.: Speciation of gas-phase and fine particle  
488 emissions from burning of foliar fuels, *Environmental Science & Technology*, 36(11), 2281-2295, doi:10.1021/es0111683,  
489 2002.

490 He, L. Y., Hu, M., Huang, X. F., Yu, B. D., Zhang, Y. H., and Liu, D. Q.: Measurement of emissions of fine particulate  
491 organic matter from Chinese cooking, *Atmos. Environ.*, 38(38), 6557-6564, doi:10.1016/j.atmosenv.2004.08.034, 2004.

492 Ho, K. F., Huang, R. J., Kawamura, K., Tachibana, E., Lee, S. C., Ho, S. S. H., Zhu, T., and Tian, L.: Dicarboxylic  
493 acids, ketocarboxylic acids, alpha-dicarbonyls, fatty acids and benzoic acid in PM<sub>2.5</sub> aerosol collected during  
494 CAREBeijing-2007: an effect of traffic restriction on air quality, *Atmos Chem Phys*, 15(6), 3111-3123, doi:10.5194/acp-  
495 15-3111-2015, 2015.

496 Hou, X. M., Zhuang, G. S., Sun, Y., and An, Z. S.: Characteristics and sources of polycyclic aromatic hydrocarbons  
497 and fatty acids in PM<sub>2.5</sub> aerosols in dust season in China, *Atmos. Environ.*, 40(18), 3251-3262,  
498 doi:10.1016/j.atmosenv.2006.02.003, 2006.

499 Huang, D. D., Zhu, S. H., An, J. Y., Wang, Q. Q., Qiao, L. P., Zhou, M., He, X., Ma, Y. G., Sun, Y. L., Huang, C., Yu,  
500 J. Z., and Zhang, Q.: Comparative Assessment of Cooking Emission Contributions to Urban Organic Aerosol Using Online  
501 Molecular Tracers and Aerosol Mass Spectrometry Measurements, *Environmental Science & Technology*, 55(21), 14526-  
502 14535, doi:10.1021/acs.est.1c03280, 2021.

503 Huang, X. Q., Han, D. M., Cheng, J. P., Chen, X. J., Zhou, Y., Liao, H. X., Dong, W., and Yuan, C.: Characteristics

504 and health risk assessment of volatile organic compounds (VOCs) in restaurants in Shanghai, *Environ Sci Pollut R*, 27(1),  
505 490-499, doi:10.1007/s11356-019-06881-6, 2020.

506 Kanakidou, M., Seinfeld, J. H., Pandis, S. N., Barnes, I., Dentener, F. J., Facchini, M. C., Van Dingenen, R., Ervens,  
507 B., Nenes, A., Nielsen, C. J., Swietlicki, E., Putaud, J. P., Balkanski, Y., Fuzzi, S., Horth, J., Moortgat, G. K., Winterhalter,  
508 R., Myhre, C. E. L., Tsigaridis, K., Vignati, E., Stephanou, E. G., and Wilson, J.: Organic aerosol and global climate  
509 modelling: a review, *Atmos Chem Phys*, 5, 1053-1123, doi:10.5194/acp-5-1053-2005, 2005.

510 Kawamura, K., Tachibana, E., Okuzawa, K., Aggarwal, S. G., Kanaya, Y., and Wang, Z. F.: High abundances of water-  
511 soluble dicarboxylic acids, ketocarboxylic acids and alpha-dicarbonyls in the mountaintop aerosols over the North China  
512 Plain during wheat burning season, *Atmos Chem Phys*, 13(16), 8285-8302, doi:10.5194/acp-13-8285-2013, 2013.

513 Lee, S., Liu, W., Wang, Y. H., Russell, A. G., and Edgerton, E. S.: Source apportionment of PM<sub>2.5</sub>: Comparing PMF  
514 and CMB results for four ambient monitorin sites in the southeastern United States, *Atmos. Environ.*, 42(18), 4126-4137,  
515 doi:10.1016/j.atmosenv.2008.01.025, 2008.

516 Li, L., Wu, D., Chang, X., Tang, Y., Hua, Y., Xu, Q. C., Deng, S. H., Wang, S. X., and Hao, J. M.: Polar organic aerosol  
517 tracers in two areas in Beijing-Tianjin-Hebei region: Concentration comparison before and in the sept. Third Parade and  
518 sources, *Environ. Pollut.*, 270, doi:10.1016/j.envpol.2020.116108, 2021.

519 Li, R., Wang, Q. Q., He, X., Zhu, S. H., Zhang, K., Duan, Y. S., Fu, Q. Y., Qiao, L. P., Wang, Y. J., Huang, L., Li, L.,  
520 and Yu, J. Z.: Source apportionment of PM<sub>2.5</sub> in Shanghai based on hourly organic molecular markers and other source  
521 tracers, *Atmos Chem Phys*, 20(20), 12047-12061, doi:10.5194/acp-20-12047-2020, 2020.

522 Makkonen, U., Virkkula, A., Mantykentta, J., Hakola, H., Keronen, P., Vakkari, V., and Aalto, P. P.: Semi-continuous  
523 gas and inorganic aerosol measurements at a Finnish urban site: comparisons with filters, nitrogen in aerosol and gas phases,  
524 and aerosol acidity, *Atmos Chem Phys*, 12(12), 5617-5631, doi:10.5194/acp-12-5617-2012, 2012.

525 Moise, T., and Rudich, Y.: Reactive uptake of ozone by aerosol-associated unsaturated fatty acids: Kinetics,  
526 mechanism, and products, *J. Phys. Chem. A*, 106(27), 6469-6476, doi:10.1021/jp025597e, 2002.

527 Nah, T., Kessler, S. H., Daumit, K. E., Kroll, J. H., Leone, S. R., and Wilson, K. R.: Influence of Molecular Structure  
528 and Chemical Functionality on the Heterogeneous OH-Initiated Oxidation of Unsaturated Organic Particles, *J. Phys. Chem.*  
529 *A*, 118(23), 4106-4119, doi:10.1021/jp502666g, 2014.

530 Nicolosi, E. M. G., Quincey, P., Font, A., and Fuller, G. W.: Light attenuation versus evolved carbon (AVEC) - A new  
531 way to look at elemental and organic carbon analysis, *Atmos. Environ.*, 175, 145-153, doi:10.1016/j.atmosenv.2017.12.011,  
532 2018.

533 Norris, G., Duvall, R., Brown, S., and Bai, S.: EPA Positive Matrix Factorization (PMF) 5.0 Fundamentals and User  
534 Guide, 2014.

535 Oliveira, C., Pio, C., Alves, C., Evtugina, M., Santos, P., Goncalves, V., Nunes, T., Silvestre, A. J. D., Palmgren, F.,  
536 Wahlin, P., and Harrad, S.: Seasonal distribution of polar organic compounds in the urban atmosphere of two large cities  
537 from the North and South of Europe, *Atmos. Environ.*, 41(27), 5555-5570, doi:10.1016/j.atmosenv.2007.03.001, 2007.

538 Pei, B., Cui, H. Y., Liu, H., and Yan, N. Q.: Chemical characteristics of fine particulate matter emitted from commercial  
539 cooking, *Front Env Sci Eng*, 10(3), 559-568, doi:10.1007/s11783-016-0829-y, 2016.

540 Pleik, S., Spengler, B., Schafer, T., Urbach, D., Luhn, S., and Kirsch, D.: Fatty Acid Structure and Degradation  
541 Analysis in Fingerprint Residues, *J. Am. Soc. Mass. Spectrom.*, 27(9), 1565-1574, doi:10.1007/s13361-016-1429-6, 2016.

542 Ren, H. X., Xue, M., An, Z. J., Zhou, W., and Jiang, J. K.: Quartz filter-based thermal desorption gas chromatography  
543 mass spectrometry for in-situ molecular level measurement of ambient organic aerosols, *J. Chromatogr. A*, 1589, 141-148,  
544 doi:10.1016/j.chroma.2019.01.010, 2019.

545 Ringuet, J., Leoz-Garziandia, E., Budzinski, H., Villenave, E., and Albinet, A.: Particle size distribution of nitrated

546 and oxygenated polycyclic aromatic hydrocarbons (NPAHs and OPAHs) on traffic and suburban sites of a European  
547 megacity: Paris (France), *Atmos Chem Phys*, 12(18), 8877-8887, doi:10.5194/acp-12-8877-2012, 2012.

548 Rogge, W. F., Hildemann, L. M., Mazurek, M. A., Cass, G. R., and Simoneit, B.: Sources of fine organic aerosol. 4.  
549 Particulate abrasion products from leaf surfaces of urban plants, *Environmental Science & Technology*, 27(13), 2700-2711,  
550 1993.

551 Rogge, W. F., Medeiros, P. M., and Simoneit, B. R. T.: Organic marker compounds for surface soil and fugitive dust  
552 from open lot dairies and cattle feedlots, *Atmos. Environ.*, 40(1), 27-49, doi:10.1016/j.atmosenv.2005.07.076, 2006.

553 Schauer, C., Niessner, R., and Poschl, U.: Polycyclic aromatic hydrocarbons in urban air particulate matter: Decadal  
554 and seasonal trends, chemical degradation, and sampling artifacts, *Environmental Science & Technology*, 37(13), 2861-  
555 2868, doi:10.1021/es034059s, 2003.

556 Schauer, J. J., Kleeman, M. J., Cass, G. R., and Simoneit, B. R. T.: Measurement of emissions from air pollution  
557 sources. 3. C-1-C-29 organic compounds from fireplace combustion of wood, *Environmental Science & Technology*, 35(9),  
558 1716-1728, doi:10.1021/es001331e, 2001.

559 Schauer, J. J., Kleeman, M. J., Cass, G. R., and Simoneit, B. R. T.: Measurement of emissions from air pollution  
560 sources. 4. C-1-C-27 organic compounds from cooking with seed oils, *Environmental Science & Technology*, 36(4), 567-  
561 575, doi:10.1021/es002053m, 2002.

562 Simoneit, B. R. T.: Biomass burning - A review of organic tracers for smoke from incomplete combustion, *Appl.*  
563 *Geochem.*, 17(3), 129-162, doi:10.1016/S0883-2927(01)00061-0, 2002.

564 Thornberry, T., and Abbatt, J. P. D.: Heterogeneous reaction of ozone with liquid unsaturated fatty acids: detailed  
565 kinetics and gas-phase product studies, *PCCP*, 6(1), 84-93, doi:10.1039/b310149e, 2004.

566 Tian, J. R., Qi, D. S., Wan, C., Liu, S. X., Wu, D. T., Qin, W., Dong, H. M., and Zhang, Q.: Quality assessment of  
567 frying oil using short-chain fatty acid profile and infrared spectrum coupled with partial least squares, *J Food Meas Charact.*  
568 14(4), 2289-2299, doi:10.1007/s11694-020-00476-3, 2020.

569 Vesna, O., Sax, M., Kalberer, M., Gaschen, A., and Ammann, M.: Product study of oleic acid ozonolysis as function  
570 of humidity, *Atmos. Environ.*, 43(24), 3662-3669, doi:10.1016/j.atmosenv.2009.04.047, 2009.

571 Wang, Q., Shao, M., Zhang, Y., Wei, Y., Hu, M., and Guo, S.: Source apportionment of fine organic aerosols in Beijing,  
572 *Atmos Chem Phys*, 9(21), 8573-8585, doi:10.5194/acp-9-8573-2009, 2009.

573 Wang, Q. Q., He, X., Huang, X. H. H., Griffith, S. M., Feng, Y. M., Zhang, T., Zhang, Q. Y., Wu, D., and Yu, J. Z.:  
574 Impact of Secondary Organic Aerosol Tracers on Tracer-Based Source Apportionment of Organic Carbon and PM<sub>2.5</sub>: A  
575 Case Study in the Pearl River Delta, China, *Acs Earth Space Chem*, 1(9), 562-571,  
576 doi:10.1021/acsearthspacechem.7b00088, 2017.

577 Wang, Q. Q., He, X., Zhou, M., Huang, D. D., Qiao, L. P., Zhu, S. H., Ma, Y. G., Wang, H. L., Li, L., Huang, C.,  
578 Huang, X. H. H., Xu, W., Worsnop, D., Goldstein, A. H., Guo, H., and Yu, J. Z.: Hourly Measurements of Organic Molecular  
579 Markers in Urban Shanghai, China: Primary Organic Aerosol Source Identification and Observation of Cooking Aerosol  
580 Aging, *Acs Earth Space Chem*, 4(9), 1670-1685, doi:10.1021/acsearthspacechem.0c00205, 2020.

581 Wang, Q. Q., and Yu, J. Z.: Ambient Measurements of Heterogeneous Ozone Oxidation Rates of Oleic, Elaidic, and  
582 Linoleic Acid Using a Relative Rate Constant Approach in an Urban Environment, *Geophys. Res. Lett.*, 48(19),  
583 doi:10.1029/2021GL095130, 2021.

584 Yee, L. D., Isaacman-VanWertz, G., Wernis, R. A., Meng, M., Rivera, V., Kreisberg, N. M., Hering, S. V., Bering, M.  
585 S., Glasius, M., Upshur, M. A., Be, A. G., Thomson, R. J., Geiger, F. M., Offenberg, J. H., Lewandowski, M., Kourtchev,  
586 I., Kalberer, M., de Sa, S., Martin, S. T., Alexander, M. L., Palm, B. B., Hu, W. W., Campuzano-Jost, P., Day, D. A., Jimenez,  
587 J. L., Liu, Y. J., McKinney, K. A., Artaxo, P., Viegas, J., Manzi, A., Oliveira, M. B., de Souza, R., Machado, L. A. T., Longo,



588 K., and Goldstein, A. H.: Observations of sesquiterpenes and their oxidation products in central Amazonia during the wet  
589 and dry seasons, *Atmos Chem Phys*, 18(14), 10433-10457, doi:10.5194/acp-18-10433-2018, 2018.

590 Zahardis, J., and Petrucci, G. A.: The oleic acid-ozone heterogeneous reaction system: products, kinetics, secondary  
591 chemistry, and atmospheric implications of a model system - a review, *Atmos Chem Phys*, 7, 1237-1274, doi:10.5194/acp-  
592 7-1237-2007, 2007.

593 Zhang, K., Yang, L. M., Li, Q., Li, R., Zhang, D. P., Xu, W., Feng, J. L., Wang, Q. Q., Wang, W., Huang, L., Yaluk, E.  
594 A., Wang, Y. J., Yu, J. Z., and Li, L.: Hourly measurement of PM<sub>2.5</sub>-bound nonpolar organic compounds in Shanghai:  
595 Characteristics, sources and health risk assessment, *Sci. Total Environ.*, 789, doi:10.1016/j.scitotenv.2021.148070, 2021.

596 Zhang, N., Han, B., He, F., Xu, J., Zhao, R. J., Zhang, Y. J., and Bai, Z. P.: Chemical characteristic of PM<sub>2.5</sub> emission  
597 and inhalational carcinogenic risk of domestic Chinese cooking, *Environ. Pollut.*, 227, 24-30,  
598 doi:10.1016/j.envpol.2017.04.033, 2017a.

599 Zhang, Q., Ning, Z., Shen, Z. X., Li, G. L., Zhang, J. K., Lei, Y. L., Xu, H. M., Sun, J., Zhang, L. M., Westerdahl, D.,  
600 Gali, N. K., and Gong, X. S.: Variations of aerosol size distribution, chemical composition and optical properties from  
601 roadside to ambient environment: A case study in Hong Kong, China, *Atmos. Environ.*, 166, 234-243,  
602 doi:10.1016/j.atmosenv.2017.07.030, 2017b.

603 Zhang, Y. X., Schauer, J. J., Zhang, Y. H., Zeng, L. M., Wei, Y. J., Liu, Y., and Shao, M.: Characteristics of particulate  
604 carbon emissions from real-world Chinese coal combustion, *Environmental Science & Technology*, 42(14), 5068-5073,  
605 doi:10.1021/es7022576, 2008.

606 Zhang, Y. X., Shao, M., Zhang, Y. H., Zeng, L. M., He, L. Y., Zhu, B., Wei, Y. J., and Zhu, X. L.: Source profiles of  
607 particulate organic matters emitted from cereal straw burnings, *J Environ Sci*, 19(2), 167-175, doi:10.1016/S1001-  
608 0742(07)60027-8, 2007.

609 Zhao, X. Y., Hu, Q. H., Wang, X. M., Ding, X., He, Q. F., Zhang, Z., Shen, R. Q., Lu, S. J., Liu, T. Y., Fu, X. X., and  
610 Chen, L. G.: Composition profiles of organic aerosols from Chinese residential cooking: case study in urban Guangzhou,  
611 south China, *J Atmos Chem*, 72(1), 1-18, doi:10.1007/s10874-015-9298-0, 2015.

612 Zhao, Y. L., Hu, M., Slanina, S., and Zhang, Y. H.: Chemical compositions of fine particulate organic matter emitted  
613 from Chinese cooking, *Environmental Science & Technology*, 41(1), 99-105, doi:10.1021/es0614518, 2007.

614 Ziemann, P. J.: Aerosol products, mechanisms, and kinetics of heterogeneous reactions of ozone with oleic acid in  
615 pure and mixed particles, *Faraday Discuss.*, 130, 469-490, 2005.

616